Atmos. Chem. Phys., 8, 1867–1879, 2008
www.atmos-chem-phys.net/8/1867/2008/

Atmospheric Chemistry and Physics

Observations of the effects of temperature on atmospheric HNO_3, ΣANs, ΣPNs, and NO_x: evidence for a temperature-dependent HO_x source

D. A. Day[1], **P. J. Wooldridge**[1], **and R. C. Cohen**[1,2,3]

[1]Department of Chemistry; University of California, Berkeley; Berkeley, CA, 94720, USA
[2]Department of Earth and Planetary Science; University of California, Berkeley; Berkeley, CA, 94720, USA
[3]Energy and Environment Technologies Division; Lawrence Berkeley National Laboratory; Berkeley, CA, 94720, USA

Received: 5 July 2007 – Published in Atmos. Chem. Phys. Discuss.: 26 July 2007
Revised: 19 November 2007 – Accepted: 20 February 2008 – Published: 28 March 2008

Abstract. We describe observations of atmospheric reactive nitrogen compounds including NO, NO_2, total peroxy nitrates, total alkyl nitrates, and HNO_3 and their correlation with temperature. The measurements were made at a rural location 1315 m a.s.l. on the western slope of the Sierra Nevada Mountains in California during summer of 2001. The ratio of HNO_3 to its source molecule, NO_2, and the ratio of HNO_3 to all other higher oxides of nitrogen (NO_z) both increase with increasing temperature. Analysis of these increases suggests they are due to a steep increase in OH of between a factor of 2 and 3 over the range 18–32°C. Total peroxy nitrates decrease and total alkyl nitrates increase over the same temperature range. The decrease in the total peroxy nitrates is shown to be much less than expected if the rate of thermal decomposition were the sole important factor. This observation is consistent with the increase in OH inferred from the temperature trends in the HNO_3/NO_2 ratio.

1 Introduction

Observations and models show surface concentrations of ozone generally increase with temperature (e.g. Cardelino and Chameides, 1990; Olszyna, et al., 1997; Sillman and Samson, 1995). Since predictions are that global temperatures will increase and regional heat waves will occur with increasing frequency as greenhouse gases accumulate in the atmosphere, understanding the mechanisms responsible for the temperature dependence of ozone is receiving renewed attention (e.g., Hogrefe, et al., 2004; Leung and Gustafson, 2005; Murazaki and Hess, 2006; Steiner, et al., 2006; Stevenson, et al., 2005). The correlation of high temperatures with stagnation events is one factor known to be responsible for ozone temperature correlations. Also, observations and models show that anthropogenic (Rubin, et al., 2006; Stump, et al., 1992; Welstand, et al., 2003) and biogenic (Lamb, et al., 1987; Wiedinmyer, et al., 2005) emissions of volatile organic compounds (VOC) increase with temperature. However, the temperature response of NO_x (the other major chemical precursor to ozone) and of more oxidized nitrogen compounds (peroxy nitrates, alkyl and multifunctional nitrates and HNO_3), co-products of ozone production, is much less well-established.

In a comprehensive modeling study, Sillman and Samson (1995) described calculations of NO_y ($NO_y \equiv NO + NO_2 + \Sigma RO_2NO_2 + \Sigma RONO_2 + HNO_3 + HONO + \ldots$) partitioning as a function of temperature for several locations. They discussed the role of the steep temperature dependence of the thermal decomposition rate for peroxyacetyl nitrate (PAN) on the response of ozone to temperature concluding, that "PAN chemistry appears to have an equal or greater impact than the more obvious causes of the temperatures dependence, i.e., insolation, H_2O, or increased emission of isoprene." The only corresponding experimental study of the relationship of temperature to nitrogen oxides is the study by Olszyna et al. (1997). They describe summertime observations of PAN/NO_y for a range of temperature and the contribution of NO_x, PAN, HNO_3, particulate nitrate, and total NO_z ($NO_z \equiv NO_y - NO_x$) to NO_y for two different temperatures at a rural site. They observe that, as a fraction of NO_y, PAN and NO_x decrease with temperature, HNO_3 and particulate nitrate change very little, while total NO_z and an unidentified contribution to NO_y (that they attribute as likely

Correspondence to: R. C. Cohen
(rccohen@berkeley.edu)

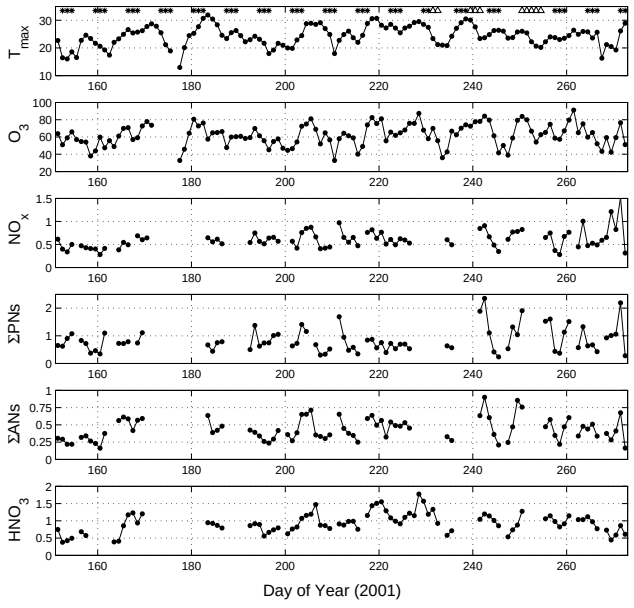

Fig. 1. Daily temperature maxima (T_{max}) and daily averages (medians) of O_3, ΣNO_{yi}, NO_x, ΣPNs, ΣANs, and HNO_3 for hours 12–16 for 1 June–30 September 2001. Symbols on top panel represent: non-weekdays (asterisks) and days where trace gas species were excluded from the analysis due to the impact of forest fires (triangles).

due to alkyl and multifunctional nitrates) increase with temperature. They suggest that the shift from PAN to the unidentified NO_z component at higher temperatures may be the result of the change in the PAN thermal equilibrium providing increased NO_x and RO_2 for alkyl and multifunctional nitrate production.

In this manuscript, we describe observations of atmospheric reactive nitrogen compounds including NO, NO_2, total peroxy nitrates (ΣPNs), total alkyl and multifunctional nitrates (ΣANs), and HNO_3 and their correlation with temperature. The measurements were made at a rural location 1315 m above sea level (a.s.l.) on the western slope of the Sierra Nevada Mountains in California during summer of 2001. The site has an extremely regular meteorology and the regional transport pattern is not strongly correlated with temperature during the summer (Dillon, et al., 2002; Murphy, et al., 2006a; Murphy, et al., 2006b and references therein). The transport pattern results in arrival of a plume originating in the city of Sacramento, CA, 80 km upwind at the University of California-Blodgett Forest Research Station (UC-BFRS) almost every day with little variation in transit time. As a consequence of this regularity, all of the observations we present are from a single source region and observations within a single season provide sufficient statistics to examine the correlations between temperature and the abundance of the various nitrogen oxides.

2 Measurements and Site Description

Measurements described in this paper were made from June–September 2001 near UC-BFRS (1315 m a.s.l., 38.9°N, 120.6°W). The site is a managed ponderosa pine plantation located in the mid Sierra Nevada Mountains 80 km northeast of Sacramento, CA (pop. 410 000, Greater Sacramento Area≅2 million) in a sparsely populated region. The climate at this site is discussed in detail in Dillon et al. (2002) and Kurpius et al. (2002). Briefly, the climate of the western Sierras has a wet and a dry season. The dry season (May–September) is characterized by warmer temperatures, low rainfall, clear skies, and steady, regular east/west, upslope/downslope winds. The wet season (October–April) is characterized by cooler temperatures, moderate rainfall or snowfall, and less regular wind patterns. Temperatures peak in summer (June–August) and are lowest in late-fall through winter. During the dry season, upslope winds of 2–3 m/s from the southwest prevail during the day, switching at the hours of 18–19 (local standard time) to downslope winds of 0.5–2 m/s from the northeast with a return to southwesterlies at 7–8 in the morning. Very few days during the dry season are an exception to this pattern. Summer measurements described in this paper were characterized by almost no precipitation (<3 cm total) and consistently warm temperatures (average daily peak ($\pm 1\sigma$)=24.4±3.7°C). Temperatures warmed by 3–5°C from early June reaching a peak in August. During summer, synoptic temperature shifts occur on timescales of 2–7 days and can have magnitudes of as much as 10°C (Fig. 1). Even in the presence of these synoptic variations, the mountain/valley wind pattern persists and results in the air at the site arriving from the west bringing with it the urban plume from the Greater Sacramento Area on more than 9 out of 10 days.

The role of transport and anthropogenic emissions in the summertime Sacramento plume, as observed at UC-BFRS, are described by Dillon et al. (2002) and Murphy et al. (2006a, b, c). Briefly, the upslope/downslope flow pattern that characterizes transport in the western Sierras imposes a regular pattern on concentrations of chemicals that have their source in the Greater Sacramento Area. The concentrations of these compounds increase throughout the day during the upslope flow from the southwest (245°). Downslope flow from the northeast (50°) returns cleaner air to the site with minimum concentrations observed in the early to mid morning. Concentrations of long-lived species (e.g. acetylene) typically begin to increase at noon and reach their peak at 22 h, 2–3 h after the shift to downslope flow suggesting the center of the plume is slightly to the north of UC-BFRS. Concentrations drop gradually after the 22 h peak reaching a minimum in mid-morning (10 AM local time). The concentrations of reactive species also exhibit strong variations with day-of-the-week due to variations in urban NO_x emissions and the resulting day-of-the-week patterns in OH concentrations (Murphy, et al., 2006b, c).

A 10 m walk-up tower was used as a sampling platform in order to sample air above the tree canopy. Gas inlets and supporting equipment were mounted on the tower. Accompanying analytical instrumentation was housed in a small wooden shed and a modified refrigerated shipping container with temperature control at the base of the tower.

Thermal dissociation-laser induced fluorescence (TD-LIF) was used to measure NO_2, total peroxy nitrates (ΣPNs), total alkyl nitrates (ΣANs), and HNO_3 at UC-BFRS. The TD-LIF technique is described in detail in Day et al. (2002) and application of the technique is described in Day et al. (2003), Murphy et al. (2006a), Rosen et al. (2004), and Cleary et al. (2007). Comprehensive details of the instrument, inlet, calibration and maintenance protocols for the measurements used in this analysis are described in Day (2003). Briefly, LIF detection of NO_2 comprises the core detection of TD-LIF (Thornton, et al., 2000). For the UC-BFRS TD-LIF instrument as set up from 2001–2005, an ambient sample flows rapidly through an inlet and is immediately split into four channels. The first one is used to observe NO_2; the second is heated to 180°C causing thermal dissociation (TD) of ΣPNs, the third to 350°C for additional TD of ΣANs, and the fourth to 550°C to include TD of HNO_3. The dissociation of all of these species produces NO_2 with unit efficiency. The NO_2 signal in each channel is the sum of the NO_2 contained in all of the compounds that dissociate at the inlet temperature or below. Differences between the NO_2 signals observed simultaneously from channels heated to adjacent set-points are used to derive absolute abundances of each of these four classes of NO_y. The technique has the advantage that it measures the total contribution to NO_y in each class. For example, ΣPNs are expected to be predominantly PAN (peroxyacetyl nitrate), PPN (peroxypropionyl nitrate), and MPAN (peroxymethacryloyl nitrate). The measurement includes these three and all other peroxy and acyl peroxy nitrates and N_2O_5. However, we do not expect non-acyl peroxy nitrates or N_2O_5 to be present in significant concentrations in the summer daytime boundary layer that is the focus of this paper. Laboratory experiments show that the HNO_3 channel measures the sum of gas phase HNO_3 and thermally labile HNO_3 aerosols such as NH_4NO_3 with near unit efficiency. Confirmation of this laboratory result with field data is available from comparisons of TD-LIF measurements and PILS aerosol nitrate measurements under conditions where NH_3 was sufficiently high that nearly 100% of the HNO_3 was aerosol NO_3^- (Fountoukis, et al., 2007). Salts such as $NaNO_3$ are not detected (Bertram and Cohen, 2003). Similarly, ΣANs are calculated to consist of all alkyl and multifunctional nitrates present in the gas or aerosol phase. Inorganic nitrate aerosols were reported to contribute 25% to total measured inorganic nitrate ($HNO_{3\ gas}$+$NO^-_{3\ particulate}$) in the mid-Sierras during summer (Zhang, et al., 2002). However, measurements of NH_3 at UC-BFRS during summer 2006 (Fischer and Littlejohn, 2007) show that concentrations are too low and temperatures too high to support NH_4NO_3 aerosol, providing an indication that any aerosol NO_3^- in the region is non-volatile and would not have been detected as part of our measurements of HNO_3. Comparison of ΣNO_{yi} ($\Sigma NO_{yi} \equiv$NO (measured by chemiluminescence)+$NO_2+\Sigma$PNs+ΣANs+HNO_3) and total NO_y (measured by catalysis – chemiluminescence) shows that these two values generally agree to within 10% (Day, et al., 2003; Dillon, 2002). Measurements of NO were made at UC-BFRS using NO-O_3 chemiluminescence (Thermo Environmental Co. model 42CTL). CO measurements were obtained using gas chromatographic separation followed by a reduction gas detector (RGA2, Trace Analytical, Inc.). Wind speed, wind direction, humidity, temperature, CO_2 and O_3 concentrations, net radiation, photosynthetically-active radiation, pressure, and VOC were measured as described in Goldstein et al. (2000), Bauer et al. (2000), and Schade et al. (2001).

3 Results and analysis

During the summer, anthropogenic emissions in the region of the study are dominated by those from motor vehicles and have a strong weekday vs. weekend variation. To eliminate this variable from our analysis, we present data from Tuesday through Friday. Observations on Saturday through Monday are consistent with our conclusions but have lower overall NO_y because of reduced weekend emissions in Sacramento and because of the approximately 2-day memory for emissions within the region (Murphy, et al., 2006b; c). Figure 1 shows the afternoon (12–16 h) medians of O_3 and the reactive nitrogen species for each day of summer 2001. Figure 2 shows the diurnal cycles of O_3, ΣNO_{yi}, NO_x, ΣPNs, ΣANs, and HNO_3 with half-hour time resolution. We represent the effects of temperature in the region by a single daily variable, the maximum temperature observed at UC-BFRS during the afternoon. We define a day as starting at 5 AM just prior to change of direction in the airflow from downslope to upslope. The blue (colder) and red (warmer) lines in Fig. 2 represent the 17th and 83rd percentile of the measurements as ordered by the associated T_{max}. The daily upslope/downslope behavior observed at this site is apparent in the diurnal cycles of ΣNO_{yi}, NO_x, ΣPNs, and O_3. During daytime, HNO_3 is much more strongly affected by photochemistry than any of these species. Its diurnal cycle more closely tracks the solar zenith angle than it does the transport patterns. This effect has been observed at many other surface sites (e.g. Brown, et al., 2004; Kleinman, et al., 1994; Lefer, et al., 1999; Parrish, et al., 1986). The pattern in the ΣANs is weak, but is closer to one that is transport dominated than one that is controlled by local photochemistry.

Figure 3 shows the median afternoon (12–16 h) $NO_x/\Sigma NO_{yi}$, ΣPNs/NO_z, ΣANs/NO_z, and HNO_3/NO_z ratios vs. T_{max}, where $NO_z \equiv \Sigma$PNs+ΣANs+HNO_3. Lines representing a least-squares fit to the data are shown.

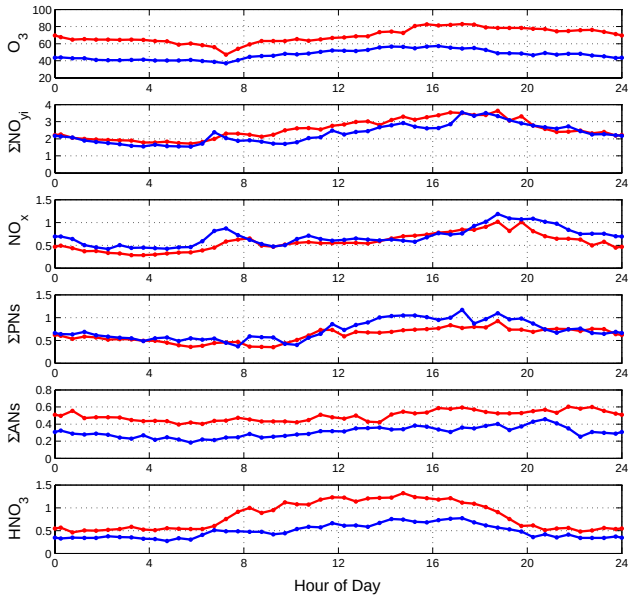

Fig. 2. Diurnal cycles of O_3, ΣNO_{yi}, NO_x, ΣPNs, ΣANs, and HNO_3 shown for half-hour intervals of the 17th and 83rd percentile of the measurements as ordered by the associated daily temperature maximum (T_{max}); T_{max} 17th percentile=20.8°C (blue), T_{max} 83rd percentile=28.4°C (red).

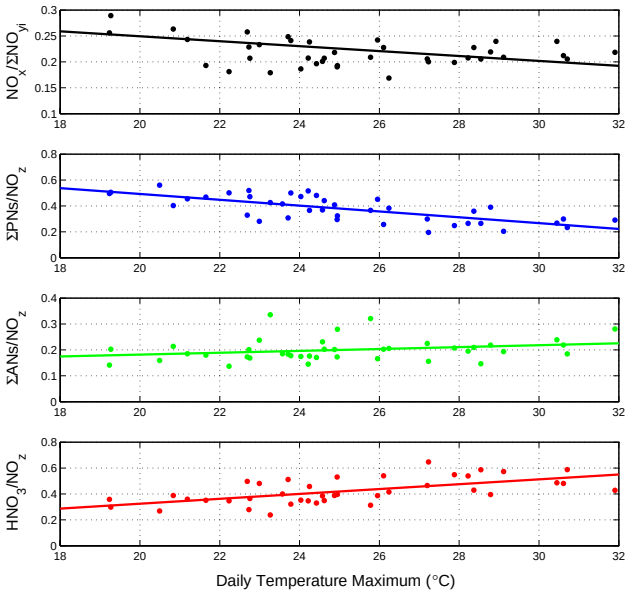

Fig. 3. $NO_x/\Sigma NO_{yi}$ $\Sigma PNs/NO_z$, $\Sigma ANs/NO_z$, and HNO_3/NO_z shown as single daily averages (medians) during hours 12–16 vs. daily temperature maximum. Best fit lines shown have parameters (from top to bottom): slopes=–0.0048, –0.023, 0.0036, 0.019 $°C^{-1}$ and R^2 values=0.14, 0.52, 0.069, and 0.37.

The correlations of $\Sigma PNs/NO_z$ (slope=–0.023 ppb/°C, R^2=0.52) and HNO_3/NO_z (slope=0.019 ppb/°C, R^2=0.37) with temperature have modest correlation coefficients and opposite signs. Both $NO_x/\Sigma NO_{yi}$ (slope=–0.0048 ppb/°C, R^2=0.14) and $\Sigma ANs/NO_z$ (slope=0.0036 ppb/°C, R^2=0.069) exhibit weaker correlations with temperature. Despite the low R^2 values, one can see that the lines shown capture the major patterns present in the data. Figure 4 shows absolute concentrations of NO_x, ΣNO_{yi}, NO_z, and O_3 vs. temperature. NO_x concentrations show no significant increase or correlation, ΣNO_{yi} and NO_z exhibit weak positive correlations and increases of approximately 25%, and O_3 shows a positive correlation with an increase of more than 30 ppb over the temperature range of 18 to 32°C.

The timing of the diurnal cycles of the individual species or classes of reactive nitrogen (Fig. 2) are similar for the two temperature ranges indicating that the major processes affecting the mixing ratios are similar, independent of temperature. The most notable trends in absolute concentration are the large increases in the HNO_3, ΣANs and O_3 with increasing temperature. In contrast, as a fraction of NO_z, the decrease in ΣPNs and the increase in HNO_3 with increasing temperature stand out more strongly than does the change in the fraction of NO_z represented by ΣANs (Fig. 3). Despite the near doubling of ΣAN mixing ratios during nights and mornings (Fig. 2) the ratio of ΣANs to NO_z during afternoon increases by only ∼30% and shows only a weak correlation with temperature (Fig. 3). NO_x/NO_y, which is often used as a surrogate for photochemical processing or age of air (e.g. Olszyna, et al., 1994; Williams, et al., 1997), also exhibits a weak negative correlation with temperature. The complementary function NO_z/NO_y has a correlation coefficient of R^2=0.14 and slope of 0.0048°C^{-1}. This correlation and slope are much smaller than reported by Olszyna et al. (1997) who describe the NO_z/NO_y correlation with temperature and indicate it has a correlation coefficient of R^2=0.81 and slope of 0.042°C^{-1}. However, at higher temperatures, where Olszyna et al. (1997) observe a larger degree of processing of the plume (NO_z/NO_y>0.7) the correlation and magnitude of slope diminishes dramatically. All but one of the observations shown in Fig. 3 have NO_z/NO_y>0.7. Thus a direct comparison of the two data sets can be misleading, as the ranges in NO_x/NO_y have little overlap.

3.1 Transport

Observations of local wind speeds and the diurnal variation duration of upslope and downslope flow do not indicate a strong correlation between warmer temperatures and the rate of mass transport from the Sacramento Valley. There was a slight but weak anti-correlation between wind speeds and temperature, which would be expected to slow the arrival of the anthropogenic plume from Sacramento. However, a decrease in windspeed could also result in decreased dilution of the plume during transport, which would result in higher concentrations of CO and NO_y when they arrive at UCBFRS. In what follows, we use observations of long-lived

anthropogenic tracers to place an upper limit on the net impact of changes in the transport times and dilution rates on plume concentrations during the fixed afternoon window.

We observe a weak correlation of CO with temperature (R^2=0.10) that corresponds to a 35% (50 ppb) increase from 18 to 32°C. In addition, long lived VOC measured at UC-BFRS for 2 months during summer 2001 (lifetime>4.5 h for OH=1×10^7 molecules/cm^3: butane, i-butane, hexane, methanol, propyne, toluene, pentane, and acetone) all had correlation coefficients of 0.10 or less with some increasing and others decreasing with temperature. While this evidence is at best equivocal, it can support no more than a 35% increase in the concentration of CO and VOC species carried by the urban plume to UC-BFRS. The best fit line for the correlation of ΣNO_{yi} vs. CO spans a range over which both compounds approximately double and has a slope of 0.0098 (R^2=0.40). This correlated range of concentrations probably represents changes in transport and mixing that are not necessarily related to temperature trends. Based on this observed correlation and the correlation of CO with temperature, temperature-dependent changes in transport and mixing can amount to no more than a 0.5 ppb (20%) increase in NO_y being transported from the Sacramento Valley to the measurement site. As this estimate pushes the CO–temperature correlation to its maximum, it is an upper limit. In addition it is likely that much of the CO increase is biogenic and not associated with NO_y making it even less likely that the temperature-dependent increases in NO_y is due to transport.

3.2 HNO_3

Each of the different classes of NO_y provides some insight into the mechanisms that are responding to changes in temperature. In this section we use the relationship between HNO_3 and its precursor, NO_2, to calculate trends in OH with temperature. HNO_3 mixing ratios vary approximately linearly with temperature for the data set increasing from 0.46 ppb at 18°C to 1.4 ppb at 32°C with a slope of 0.067 ppb/°C and an R^2=0.50. During the daytime, the concentration of the HNO_3 can be approximately described as a stationary state between chemical production and losses to deposition and dilution:

$$k_{OH+NO_2}[OH][NO_2] = \frac{V_{dep}}{H_{ml}}[HNO_3] + K_{dil}\left([HNO_3] - [HNO_3]_{bg}\right) \quad (1)$$

where V_{dep} is the deposition velocity (0.034 m/s (Farmer and Cohen, 2007), H_{ml} is the mixed layer height (~800 m; Carroll and Dixon, 1998; Dillon, et al., 2002; Seaman, et al., 1995), K_{dil} is the effective dilution rate coefficient including both vertical venting and horizontal diffusion of the plume into the background air (~0.23 h^{-1}; Dillon, et al., 2002), and $[HNO_3]_{bg}$ is the background nitric acid concentration into which the plume is diluted. We estimate that the free-tropospheric $[HNO_3]_{bg}$ for this region is roughly 200 ppt

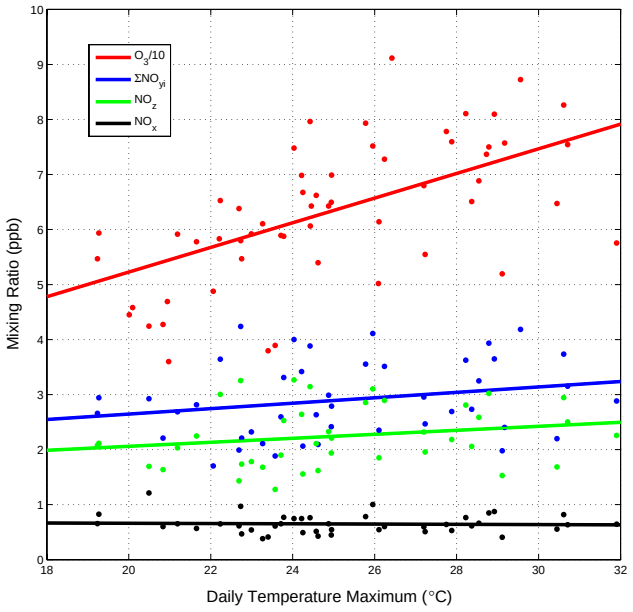

Fig. 4. O_3, ΣNO_{yi}, NO_z, and NO_x shown as single daily averages (medians) during hours 12-16 vs. daily temperature maximum. Best fit lines shown have parameters (from top to bottom): slopes=2.24, 0.049, 0.036, –0.0007 °C^{-1} and R^2 values=0.43, 0.052, 0.043, 0.002.

which is the intercept of the plot of $[HNO_3]$ vs. $[H_2O]$ for observations discussed in Murphy et al. (2006a) at a site at higher elevation in the Sierras which was often affected by free tropospheric air. Rearranging,

$$\frac{[HNO_3]}{[NO_2]} = \frac{k_{OH+NO_2}[OH] + K_{dil}[HNO_3]_{bg}/[NO_2]}{\frac{V_{dep}}{H_{ml}} + K_{dil}} \quad (2)$$

For NO_2=0.6 ppb, OH=1×10^7 molecules/cm^3 and k_{OH+NO2}=9.90×10^{-12} cm^3 molecules^{-1} s^{-1} at 25°C (Sander, et al., 2006), the lifetime of 1 ppb of HNO_3 with respect to production is approximately 5 h, the lifetime of HNO_3 with respect to deposition (τ_{dep}=H_{ml}/V_{dep}) during the day is about 6.5 h, and the lifetime of HNO_3 due to the combination of deposition and dilution is about 2.6 h. HNO_3 is produced more rapidly upwind where the $NO_2$and probably the OH concentrations are higher (Murphy, et al., 2006c) and thus, at UC-BFRS, HNO_3 concentrations are likely slightly higher than would be achieved in steady-state because the transport source of HNO_3 is significant. Nonetheless, the steady-state expression above provides a reasonable approximation for thinking about HNO_3, especially as it relates to relative changes in OH. Similar equations relating HNO_3, NO_2, and OH, without the dilution term, have been presented previously (Brown, et al., 2004; Parrish, et al., 1986).

We calculate afternoon OH concentrations using Eqs. (1) and (2) (and the values for other parameters discussed above and including the temperature dependence of the OH+NO_2

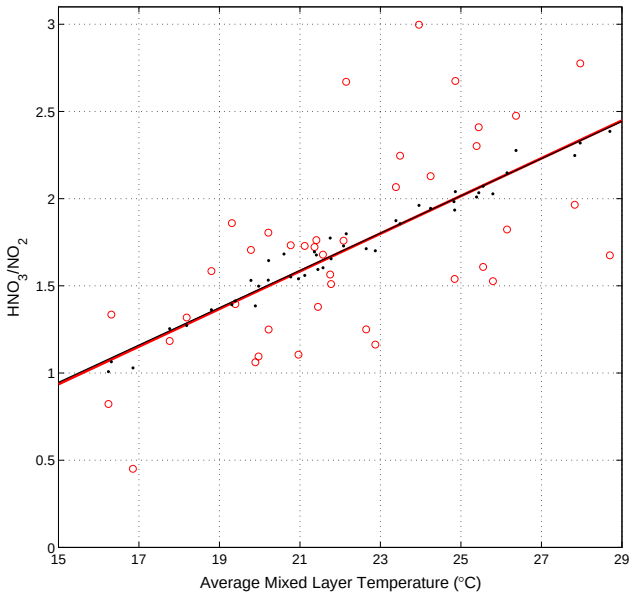

Fig. 5. HNO_3/NO_2 shown as single daily averages (medians) during hours 12–16 vs. average mixed layer temperature. Observations (red circles), modeled values (black points), and the coincident best fit lines are shown.

rate constant). We estimate the average temperature within the 800 m mixed layer (T_{ml}) using surface temperatures and a lapse rate of 6.5°C/km, resulting in effective temperatures approximately 3°C lower than surface temperatures. A linear fit of the correlation between the calculated OH and T_{ml} yields an increase in OH from 7.5×10^6 molecules/cm^3 at T_{ml}=15°C to 2.4×10^7 molecules/cm^3 at T_{ml}=29°C, a 3.2-fold increase. Figure 5 shows the median afternoon (12–16 h) HNO_3/NO_2 data vs. T_{ml} (red circles). Also shown are modeled values for the HNO_3/NO_2 ratio calculated using the linear best fit line from the OH vs. T_{ml} correlation and Eq. (2). The coincident best fit lines are also shown. The scatter in the modeled data is due solely to the NO_2 data since the other variables are either held constant or vary linearly with temperature. The linear fit captures the general trend in the HNO_3/NO_2 data suggesting that a linear relationship between OH and T is reasonable. Below we explore a number of the factors in Eq. (2) to assess how sensitive our conclusion of a strong temperature-dependent increase in OH is to parameters that are important but were not measured in this study.

Several different factors might affect the NO_2/HNO_3 ratio:

1. the mixed layer height,
2. the deposition velocity,
3. the dilution rate, and
4. the NO_2 or HNO_3 background concentrations.

We will take each of these in turn. First, we do not expect a large variation of mixed layer height with temperature in this region because the planetary boundary layer (PBL) height is more strongly defined by the dynamical forcing of the large scale circulation and the Sierra Nevada Mountains than it is by surface heating. Also, the PBL is less driven by latent heat than in other regions because of this dynamical effect and the low humidity in the region. Furthermore, the overall cloudiness in the region during the summer is so low that variations in clouds (or actinic flux) are unimportant. Data from 7 days of flights over this region of the Sierra Nevadas during summertime showed no correlation between afternoon mixing layer heights and surface temperatures (Carroll and Dixon, 1998). In that study, afternoon surface temperatures varied by 10°C and the lack of correlation was observed for the three surface elevations reported in their transect (∼150 m a.s.l., ∼550 m a.s.l., and ∼1250 m a.s.l.), roughly along the transect from the Sacramento Valley to our observation site. Although mixed layer heights did not correlate with temperature they were observed to vary substantially. Mixed layer heights ranged from 660 to 1250 m above ground level (a.g.l.) at the highest elevation location where the ground was 1250 m a.s.l., but on average only increased from ∼800 m a.g.l. above the city of Sacramento to ∼1000 m a.g.l. at the highest elevation.

Although we do not believe this to be the case, it is possible to assume the mixed layer height is correlated with temperature and then evaluate how this correlation affects the NO_2/HNO_3 ratio (and consequently the calculated OH). Assuming that H_{ml} grows linearly from 530 to 1070 m from 15 to 29°C and inserting these values into Eq. (2) results in a smaller relative change in the calculated OH over this temperature range. With this assumption, we calculate a 2.3-fold increase with T from 15 to 29°C compared to the 3.2-fold increase assuming a constant mixed layer height. With the varying boundary layer height we calculate 30% more OH at the lowest temperatures and 10% less OH at the highest temperatures as a result of changes in the relative importance of deposition to the integrated removal rate of HNO_3 in the boundary layer.

We expect the direct effect of temperature on deposition velocity will be less than 1% over this temperature range (Delphine Farmer, Personal communication). However if deposition velocity varied with temperature, the effect could have the same magnitude as changes in H_{ml}, but act the opposite direction. As shown in Eq. (2), the ratio of V_{dep}/H_{ml} controls the lifetime of HNO_3 to loss by deposition to the earth's surface. We observe a slightly negative correlation of afternoon wind speeds with temperature (a decrease of 8%), which will affect the depositional velocity roughly proportionally (Farmer, personal communication). This small shift was included in the initial calculation above, with V_{dep} varied linearly and set to 0.034 m/s at the middle of the temperature range. This had the effect of increasing OH by 3.7% at the lowest temperatures and decreasing OH by 1.3% at the

highest temperatures compared to using a fixed V_{dep}. Thus we conclude that variations in PBL height or V_{dep} will affect the numerical value of the OH increase with temperature but cannot change the basic conclusion that OH increases by 2–3-fold with temperature.

We also consider the effect of changes in dilution with temperature. The result of a linear decrease in K_{dil} by a factor of 2 over the temperature range (centered at 0.23 h^{-1} for the mid temperatures) is that the calculated OH is 35% higher at the lowest temperature and is 13% lower at the highest temperature. This represents a 2.1-fold increase in OH over the temperature range, a smaller shift than when using a fixed dilution rate coefficient. This result is nearly identical to that calculated for an increasing boundary layer height with temperature. As discussed in section 3.1, observations of CO, anthropogenic VOC, and total NO_y do not support a large shift in dilution rates. Again, changes to our assumptions about dilution do not change our basic conclusion that OH increases with temperature.

In another sensitivity test of the model we considered using a background HNO_3 more similar to our typical nighttime observations of HNO_3, ~400 ppt. The result of using 400 ppt rather than 200 ppt for $[HNO_3]_{bg}$ in Eq. (3) is an increase in calculated OH of 2.5×10^6 molecules/cm^3 that is nearly invariant with temperature. This adjustment yields a 4.3-fold increase in calculated OH (compared to 3.2 for using 200 ppt) over the temperature range. This illustrates the importance of using an accurate background HNO_3 on both the absolute OH concentrations and the relative change with temperature. However, in our opinion, our observations in the nocturnal boundary layer are affected by near-surface chemistry with production of HNO_3 from reactions of NO_3 and N_2O_5 at night and therefore the 200 ppt value determined from measurements outside the boundary layer is more representative of the background air which is being mixed into the boundary layer. Unlike that for HNO_3, the background value of NO_2 is not applicable to this model (that assumes steady-state HNO_3) since losses of NO_2 due to mixing are only relevant in so far as they affect NO_2 concentrations for which we have a direct measurement.

The more rapid conversion of NO_2 to HNO_3 implied by this higher OH must also be accompanied by additional temperature-dependent sources of NO_2 since the NO_2 remains nearly constant with variations in temperature. The total of all NO_{yi} species that we observe, ΣNO_{yi}, increases with temperature (by about 25%), a fact that is somewhat surprising since increases in HNO_3 should be associated with more rapid deposition and removal of NO_y. Likely temperature-dependent chemical sources of NO_2 include the thermal decomposition of PNs or an increase in soil NO_x emissions. These factors are discussed further in sections 3.3 and 3.5 below. A decrease in the dilution rate correlated with increases in temperature is also hypothetically possible but as discussed above likely to be a small effect.

We expect that the OH concentrations predicted using the local NO_2 and HNO_3 concentrations in the steady-state calculation are an overestimate of the OH responsible for producing the observed HNO_3 due to the fact that HNO_3 observed represents an average over 2–3 hours of production and loss upwind where NO_2 mixing ratios are higher. Without a more detailed model, estimating the effective NO_2 for use in Eqs. (1) and (2) is difficult. To bracket the amount of $NO_2$and thus the absolute value of OH we use a 3-fold larger value of NO_2 to calculate OH of 2.7×10^6 and 8×10^6 molecules/cm^3 for the two temperature extremes. Despite lowering the OH by a factor of three, the trend with temperature is still approximately a 3-fold increase. The two calculations using different NO_2 concentrations both produce OH estimates in the range of the average OH concentration in the Sacramento plume ($1.1\pm0.5\times10^7$ molecules/cm^3) that Dillon et al. (2002) calculated using a Lagrangian model and VOC measurements for the 5 h transect from Folsom, CA to UC-BFRS. That model represented a single average daily maximum temperature of 25°C.

3.3 ΣPNs

ΣPNs are approximately in thermal equilibrium with peroxyacyl radicals and NO_2 under warm boundary layer conditions (Cleary, et al., 2007):

$$K_{PN_i}(T)=\frac{[PN_i]}{[PA_i][NO_2]} \quad (3)$$

Where $K_{PN_i}(T)$ is the equilibrium constant, for each respective PN. This equilibrium is established through the reactions:

$$PA_i + NO_2 \rightarrow PN_i \quad (R1)$$

$$PN_i \rightarrow PA_i + NO_2 \quad (R2)$$

which determine the partitioning of the PN reservoir between the stable PN_i and its radical partner PA_i. In addition, peroxyacyl radicals are approximately in photochemical steady-state with their sources and sinks (Cleary, et al., 2007). Consider the case for the most common peroxyacyl nitrate, peroxyacetyl nitrate (PAN) and the peroxyacetyl radical (PA). The primary reactions that contribute to net formation and loss of the sum of PA and PAN include:

acetaldehyde or methyglyoxal + OH
$(+O_2) \rightarrow PA + H_2O$ (R3)

$$PA + NO \rightarrow \text{Products} \quad (R4)$$

$$PA + HO_2 \rightarrow \text{Products} \quad (R5)$$

$$PA + RO_2 \rightarrow \text{Products} \quad (R6)$$

Solving for the steady-state concentration of PA+PAN we derive:

$$[\text{PA+PAN}]_{ss} = \left(\frac{k_3[\text{acetaldehyde (methyglyoxal)}][\text{OH}]}{k_4[\text{NO}] + k_5[\text{HO}_2] + k_6[\text{RO}_2]}\right) (1 + K_{\text{PAN}}[\text{NO}_2]) \quad (4)$$

We estimate the average temperature within the boundary layer using surface temperatures and the environmental lapse rate as discussed above in Sect. 3.2. From 15 to 29°C the equilibrium constant controlling the ratio of PA_i to PN_i decreases by a factor of 9 for PAN and PPN (Sander, et al., 2006) whereas the observed ratio of ΣPNs/NO_2 decreased by less than a factor of 2. Using the observed ΣPN and NO_2 concentrations and the equilibrium constant for PAN, we calculate the sum of all peroxyacyl radicals during mid-afternoon in the boundary layer. This calculation yields a 5–6-fold increase in peroxyacyl radicals from ~0.7 ppt to 3.7 ppt for the 15–29°C range of boundary layer average temperature. Trainer et al. (1991) examined observations at Scotia, PA in the summertime and calculated an increase in peroxyacyl radicals from 8 to 14 ppt over the temperature range 26–32°C.

Since all of the losses of PA+PN are through the reactions of the radical, if all other factors were constant, this increase in PA radical concentrations implies a roughly 5–6-fold increase in the loss rate of ΣPNs during transport to UC-BFRS. The decrease we observe is much smaller, only about 30%, a fact that implies a nearly 5–6-fold increase in the source of ΣPNs. Two factors are primarily responsible:

1. A doubling of acetaldehyde, an implied increase of methylglyoxal associated with increased isoprene emissions and oxidation, and an increase of methacrolein with temperature. These represent increases in sources of two of the major peroxyacyl radicals. Isoprene and methacrolein were both shown to increase by a factor of ~10-15 over the temperature range considered in our study (Dreyfus et al., 2002). The increases reported by Dreyfus et al. were computed using summertime data spanning 9–17 h (upslope flow only) and therefore may be influenced by the diurnal cycle in transport. Calculating these relationships using single daily averages of afternoon observations (made at UC-BFRS during a 2-month summer intensive from mid-July to mid-September, 2001) yields substantially smaller relative increases in isoprene and methacrolein over this temperature range (~6-fold and ~3-fold, respectively).
2. A large increase in OH.

If we assume a 3-fold increase in OH and a 2-fold increase in ΣPN source aldehydes then the product is equal to the 6-fold increase in sources that we calculate and is consistent with the increase in OH estimate from the HNO_3/NO_2 ratio.

The net ΣPN decrease with T that we observe at UC-BFRS corresponds to a release of about 500 ppt of NO_2 during transit to the site. However, at UC-BFRS we observe a negligible change in NO_x with temperature implying almost all of this 500 ppt has gone to increases in the HNO_3 (and ΣAN) production during the transit of the plume to UC-BFRS.

3.4 ΣANs

ΣANs increase by 250 ppt (75%) with temperature (Fig. 2) and by 45% and 30% as a fraction of NO_y and NO_z (Fig. 3), respectively. Quantitative interpretation of these increases is difficult because VOC precursors and their oxidation rates due to reaction with OH are both increasing. In addition, the lifetime of ΣANs with respect to OH and O_3 is highly uncertain because it is not known what fraction of reactions of OH with ΣANs produce multifunctional ΣAN products and what fraction produce NO_2 or HNO_3 (see Farmer and Cohen (2007) for additional discussion of this issue). Inspection of the diurnal cycle of ΣANs in Fig. 2 suggests that ΣAN increases may, in part, be due to nighttime chemical production. Evaluation of the effects of temperature on nighttime chemistry is interesting, but beyond the scope of this manuscript.

3.5 NO_x and NO_y

In addition to the effects of ΣPNs or decreased dilution rates discussed above, an increase in the source of NO_x with temperature may be explained by increased NO_x soil emissions. Herman et al. reported that NO_x soil emissions in an oak forest in the Sierra Nevada foothills had fluxes of 5.8–15 ppt m s^{-1} (under canopy/open area with mean soil temperatures of ~24/28°C) (2003). Farmer and Cohen use an observationally constrained model to calculate a NO_x flux from UC-BFRS of 27 ppt m s^{-1} (2007). That NO_x flux was estimated to be no more than 1/3 due to soil emissions with the balance likely HONO emissions or due to an unknown source. Soil NO_x emissions have been shown to exhibit an exponential relationship with temperature (van Dijk et al., 2002; Williams et al., 1992). The estimated soil term of 9 ppt m s^{-1}, diluted into an 800 m boundary layer, represents ~40 ppt/h . Over a 5 h transit time, these emissions could account for a large fraction of the source that maintains near constant NO_x and of the approximately 700 ppt increase in NO_y that we observe. Thus, if the emissions are an exponential function of temperature, they are of a magnitude that would explain the temperature dependence of the NO_x observations.

The ratio of NO/NO_2 during mid-afternoon showed a weak correlation with temperature (slope=–0.0020°C^{-1}, R^2=0.063, increasing by about 17% from 18 to 32°C)). This ratio is controlled by the photolysis of NO_2 and oxidation of NO by oxidants such as O_3, HO_2 and RO_2. A rapid steady-state is established during midday at locations removed from

large NO_x sources that can be represented as:

$$j_{NO_2}[NO_2]= k_{NO+O_3}[NO][O_3]+k_{NO+RO_2}[NO][HO_2+RO_2] \quad (5)$$

where j_{NO_2} is the rate constant of the photolysis reaction $NO_2 + h\nu \rightarrow NO+O$. (UCAR/NCAR/ACD), k_{NO+O_3} the rate constant for the reaction of $NO+O_3 \rightarrow NO_2+O_2$ (Sander et al., 2006), and k_{NO+RO_x} the average rate constant for the reactions $NO+RO_2 \rightarrow NO_2+RO$ and $NO+HO_2 \rightarrow NO_2+OH$ which we approximate as the rate constant for reaction of HO_2 with NO. Rate constants are taken from Sander et al. (2006). During this summertime study cloudiness was very low (as is typical) and therefore we expect calculated values of j_{NO_2} to be a good approximation of the local actinic flux.

For the days that we have simultaneous measurements of NO, NO_2 and O_3 we estimate the $[HO_2+RO_2]$ concentration using Eq. (5). The afternoon averages were 200 ppt with a 100 ppt variance. However, the $[HO_2+RO_2]$ values derived from the NO/NO_2 ratio is quite noisy and affected substantially by uncertainty in the NO instrument's measurement of zero. Within the envelope of the noise and our estimates of the effects of the uncertainty in the NO instrument zero, we estimate the maximum trend in peroxy radicals that would be consistent with the data is +47% and the minimum is –25% (95% confidence interval). This is a weaker temperature dependence than suggested by our interpretation of the HNO_3 and ΣPN data. Conservative estimates of OH increases of 2–3-fold, as inferred above, would normally be accompanied by $[HO_2+RO_2]$ increases of 40–200% assuming that peroxy radicals increase with OH concentration with a dependence between the square root and linear. We derive these two limits for the $[HO_2+RO_2]$ vs. OH relationship from steady-state approximations ($P_{[HO_2+RO_2]}=L_{[HO_2+RO_2]}$) for NO_x-limited conditions ($k_{HO_x+HO_x}[HO_x][HO_x] \approx [OH][VOC]$) and for VOC-limited conditions ($k_{HO_x+NO}[HO_2]][NO] \approx [OH][VOC]$ and $[RO_2] \approx [HO_2]$), respectively. Considering that local conditions at UC-BFRS are likely fairly NO_x-limited, the lower end of the 40–200% range is probably more reasonable. The lack of a large increase in $[HO_2+RO_2]$ (only a slight overlap with the predicted increase assuming large local OH increases) probably reflects both the persistence of NO_x-limited conditions and the fact that most of the increase in OH occurred upwind, perhaps in closer proximity to the isoprene emissions. Additionally, it may be an indication that a chemical process that alters the $[HO_2+RO_2]$ to OH ratio is active.

3.6 O_3

The positive correlation of O_3 with temperature shown in Fig. 4 is typical for a rural site. This slope of 2.2 ppb/°C is similar to that reported for other rural sites at a similar temperature range (3±1, ~3–5, respectively)(Olszyna, et al., 1997; Sillman and Samson, 1995) and is slightly higher (~3 ppb/°C) if peak ozone rather than the early afternoon average is used (as was used in the calculation of Sillman and Samson, 1995). Inspection of the diurnal cycles of O_3, shown in Fig. 2, suggests that this relationship with temperature is due both to increases in production rates for single days and to accumulation during multi-day events where carryover from the previous day is important.

4 Discussion

Our results bear some similarities to the results of Olszyna et al. (1997), who report that, over an ambient temperature from 25°C to 30°C, the ratio PAN/NO_y decreased with a slope of $-0.015°C^{-1}$, that NO_z/NO_y increased from 55 to 75%, that NO_x/NO_y decreased from 45 to 25%, that PAN/NO_y decreased from 35 to 20%, that $[HNO_3$+particulate nitrate$]/NO_y$ was unchanged, and that the "missing NO_y" increased from 0 to 20% of NO_y. We observe a slope for $\Sigma PNs/\Sigma NO_{yi}$ of $-0.015°C^{-1}$, identical to the PAN/NO_y slope reported by Olszyna et al. (1997). In contrast to the observation of Olszyna et al. (1997), we see a much larger increase in HNO_3/NO_y and, equating their "missing NO_y" with our ΣANs, we observe a much smaller increase of $\Sigma ANs/NO_y$. Other reports of correlations of reactive nitrogen species with temperature include positive correlations of HNO_3 and negative correlations of PAN for three different seasons (summer, spring, and winter) (Bottenheim and Sirois, 1996), a negative correlation of PAN and temperatures for a yearlong dataset (Gaffney and Marley, 1993), and increases of PAN with temperature during summer (Schrimpf, et al., 1998). In addition, several models discussing effects of climate change predict decreases in ΣPN concentrations (e.g., Steiner, et al., 2006; Stevenson, et al., 2005).

Since the model discussed in Sillman and Samson (1995) is the most complete and comparable discussion in the literature of the relationship of temperature and reactive nitrogen partitioning in a rural environment, it is valuable to discuss further the similarities and differences between their model and our measurements. They model rural sites in Michigan and Alabama for a summer day and describe changes in midday OH, HO_2, O_3, HNO_3, ΣPNs, ΣANs, and NO_x concentrations vs. the daily maximum temperature. For these two sites, over the temperature range we consider in this paper (18–32°C), they show relative changes in ΣPNs of –50%, ΣANs of +50% to as much +150%, and little to no change in NO_x or HNO_3. Although our observations of ΣPNs and NO_x closely match those predictions, this is likely fortuitous because of the large differences between the predictions of HNO_3 and ΣANs and our observations.

In the Sillman and Samson (1995) calculations most of the additional NO_x available from decreasing ΣPNs forms ΣANs, making ΣANs the dominant contribution to NO_z at

higher temperatures. They attribute this large rise in ΣANs to increasing isoprene emissions producing isoprene nitrates. They used a yield of 10% for alkyl nitrate formation from reaction of NO with isoprene peroxy radicals, and a slow deposition velocity for isoprene nitrates. Comparison of our observations of ΣANs on the DC-8 to a global model shows that parameters that are more consistent with the ΣANs measurements are a yield of 4% and a rapid deposition rate, one that is similar to that of HNO_3 (Horowitz, et al., 2007). Presumably, inserting these parameters in the Sillman and Samson model would result in not only decreases in ANs but also increases in NO_x (that would partially be converted to HNO_3) and thus increased HNO_3 at higher temperatures.

Nevertheless, it is surprising that Sillman and Samson (1995) predict nearly constant HNO_3 since they show predicted changes in OH (for the Michigan site) in which OH nearly doubles over the relevant temperature range. Since no significant increase in HNO_3 accompanies this OH increase, the formation rate of ANs, consuming the available NO_x, must increase much faster in the model – presumably because isoprene is a more effective NO_x sink in the model than at our site. Also in contrast to our observations, other researchers have predicted that with increased isoprene, PNs (and ANs) will increase at the expense of HNO_3 (Lopez, et al., 1989; Trainer, et al., 1991). Further research is needed to understand if these differences between models and our observations reflect different local or regional conditions or if they provide a generally useful diagnostic for temperature-dependent atmospheric chemistry.

Increases in OH with high temperature were predicted by Sillman and Samson (1995), who showed they would be due to a combination of increases in O_3, H_2O, and solar radiation in the Eastern U.S. At UC-BFRS, there is no significant increase in H_2O concentration nor photosynthetically-active radiation with temperature (R^2=0.005, 0.026, respectively); O_3increases by 70% from 18 to 32°C (Fig. 4) and, if only considering the effect of the primary production rate of OH (O_3+h$\nu\rightarrow$ 2OH), this would account for an increase in OH of 70%.

We can remove this effect of O_3 on OH concentrations by normalizing the calculated OH to O_3 concentrations and plotting versus temperature. This results in a diminished correlation (R^2=0.24 rather than 0.45) and a smaller relative increase (2.2 as opposed to 3.2-fold). The significance of this estimated increase in OH can be assessed by considering the uncertainty in the best-fit line which is ±28% (1σ) equivalent to a relative increase over the temperature range between 1.4-fold and 4.0-fold for a 95% confidence interval. This implies that the estimated increase in OH not directly associated with production from ozone is significant if there are not other large systematic shifts in the values in Eq. (2) used for the OH calculation. In fact, using Eq. (2) we calculate that a factor >2 increase in the mixed-layer height or ∼2 decrease in the mixing rate coefficient with temperature would be necessary to shift the correlation of ozone-normalized OH vs. T and decrease the slope enough to bring a zero slope line within the 95% confident interval. In order for the actual calculated slope to be zero, these shifts would need to be factors of magnitude ∼7 and ∼6, respectively. For reasons discussed in sections 3.1 and 3.2 shifts in these parameters as large as a factor of 2 are very unlikely.

A likely more important factor is the increase in upwind sources of isoprene and its oxidation products which are exponentially related to temperature, increasing by factors of 3-15 over the range 18-32°C (this study; Dreyfus, et al., 2002). There are now several direct observations of OH and indirect measures of the influence of OH showing that OH is increased above model predictions in environments rich in biogenic VOC (Farmer and Cohen, 2007; Kuhn, et al., 2007; Ren, et al., 2007; Tan, et al., 2001). CH_2O, which is calculated to be nearly equal in importance to O_3 as a HO_x source at UC-BFRS (Pérez and Cohen, 2008[1]) is a major product of isoprene oxidation and could account for part of the inferred increase in OH with temperature. However, calculations by Pérez and Cohen (2008) show that increases in H_2CO are likely too small to account for the increase in its entirety, leading us to suggest that there are chemical processes associated with isoprene emissions (and thus indirectly with temperature) that are not accurately represented in current chemical mechanisms. This conjecture is consistent with the analysis of Thornton et al. (2002) and more recent laboratory and field data (Hasson, et al., 2004; Kuhn, et al., 2007; Ren, et al., 2007; Stickler, et al., 2007).

5 Conclusions

We have presented measurements of the effects of ambient temperature (18–32°C) on the atmospheric mixing ratios of a nearly complete suite of speciated reactive nitrogen. We observe that there is a small decrease in NO_x/NO_y, a large increase in HNO_3/NO_2, a decrease in ΣPNs and an increase in ΣANs with increasing temperature. Analysis of the results show small changes in NO_x and ΣNO_{yi} indicating a near balance in temperature-dependent NO_x sources, NO_x oxidation rates, and permanent NO_z losses in relatively aged air. However, large changes in the ratios of the different reactive nitrogen compounds suggest a large temperature-dependent increase in OH. This increase cannot be explained by temperature-dependent increases in O_3, H_2O, or actinic flux, indicating that other temperature-dependent processes, likely related to emission of biogenic VOCs such as isoprene, exert important controls over OH.

There are few measurements of the effects of temperature on NO_y speciation where there were sufficient observations to track the nitrogen budget. The one prior measurement that was nearly as comprehensive as the one described here

[1] Pérez, I. M. and Cohen, R. C.: Calculations of the chemical composition during transport of the Sacramento urban plume, in preparation, 2008.

was much closer to the source region, and thus there is little overlap of the NO_x/NO_y ratio (or approximate photochemical age) of the two data sets. Still, the results are similar in the region of overlap suggesting that our results might be representative of many locations and not special because of their location in the foothills of the Sierra Nevada downwind of Sacramento. Our results are quite different than prior model calculations. We observe a larger increase in the contribution of HNO_3 to NO_z and to NO_y with temperature and a smaller increase in alkyl nitrates than predicted by in Sillman and Samson (1995). The latter of these is probably in part due to the high yield (10%) and low deposition velocity of isoprene-derived alkyl nitrates used in that model, whereas there is growing evidence suggesting that smaller yields and more rapid deposition velocities for isoprene nitrates are what is occurring in the atmosphere.

In light of these and other improvements in our understanding of atmospheric chemistry, it would be valuable to revisit the temperature dependence of precursors to ozone more systematically in current models. This would help to assess whether models are consistent with the observations of NO_{yi} and inferences about OH and other HO_x components presented herein and also our current understanding of the likely effects of climate change on air quality.

Acknowledgements. We gratefully acknowledge support for the observations by the NASA Instrument Incubator Program under Contract #NAS1-99053 and support for the analysis by the US Environmental Protection Agency through grant RD-83096401-0 to the University of California, Berkeley. Although the research described in this article has been funded wholly or in part by the US Environmental Protection Agency through grant RD-83096401-0 to the University of California, Berkeley, it has not been subjected to the Agency's required peer and policy review and therefore does not necessarily reflect the views of the Agency and no official endorsement should be inferred. We also thank the staff of UC-BFRS for their support and SPI for access to the research site.

Edited by: A. Hofzumahaus

References

Bauer, M. R., Hultman, N. E., Panek, J. A., and Goldstein, A. H.: Ozone deposition to a ponderosa pine plantation in the Sierra Nevada Mountains (CA): a comparison of two different climatic years, J. Geophys. Res.-A., 105, 22 123-22136, 2000.

Bertram, T. H. and Cohen, R. C.: A prototype instrument for the real time detection of semi-volatile organic and inorganic nitrate aerosol, Eos Trans. AGU, 84(46), Fall Meet. Suppl., Abstract A51F-0740, 2003.

Bottenheim, J. W. and Sirois, A.: Long-term daily mean mixing ratios of O_3, PAN, HNO_3, and particle nitrate at a rural location in Eastern Canada - Relationships and implied ozone production efficiency, J. Geophys. Res.-A., 101, 4189–4204, 1996.

Brown, S. S., Dibb, J. E., Stark, H., Aldener, M., Vozella, M., Whitlow, S., Williams, E. J., Lerner, B. M., Jakoubek, R., Middlebrook, A. M., DeGouw, J. A., Warneke, C., Goldan, P. D., Kuster, W. C., Angevine, W. M., Sueper, D. T., Quinn, P. K., Bates, T. S., Meagher, J. F., Fehsenfeld, F. C., and Ravishankara, A. R.: Nighttime removal of NO_x in the summer marine boundary layer, Geophys. Res. Lett., 31, L07108, doi:10.1029/2004GL019412, 2004.

Cardelino, C. A. and Chameides, W. L.: Natural hydrocarbons, urbanization, and urban ozone, J. Geophys. Res.-A., 95, 13 971–13 979, 1990.

Carroll, J. J. and Dixon, A. J.: Tracking the Sacramento pollutant plume over the western Sierra Nevada. Final Report to California Air Resources Board under Interagency Agreement #94-334. 26 pages plus appendicies., http://www.arb.ca.gov/research/apr/past/atmospheric.htm, 1998.

Cleary, P. A., Wooldridge, P. J., Millet, D. B., McKay, M., Goldstein, A. H., and Cohen, R. C.: Observations of total peroxy nitrates and aldehydes: measurement interpretation and inference of OH radical concentrations, Atmos. Chem. Phys., 7, 1947–1960, 2007, http://www.atmos-chem-phys.net/7/1947/2007/.

Day, D. A.: Observations of NO_2, total peroxy nitrates, total alkyl nitrates, and HNO_3 in the mid-Sierras and Sacramento Plume using thermal dissociation – laser induced fluorescence, Ph. D. thesis, 207 pp., University of California at Berkeley, Berkeley, Ca, 2003.

Day, D. A., Dillon, M. B., Wooldridge, P. J., Thornton, J. A., Rosen, R. S., Wood, E. C., and Cohen, R. C.: On alkyl nitrates, O_3, and the "missing NO_y", J. Geophys. Res.-A., 108, 4501, doi:10.1029/2003JD003685, 2003.

Day, D. A., Wooldridge, P. J., Dillon, M. B., Thornton, J. A., and Cohen, R. C.: A thermal dissociation laser-induced fluorescence instrument for in situ detection of NO_2, peroxy nitrates, alkyl nitrates, and HNO_3, J. Geophys. Res.-A., 107, 4046, doi:10.1029/2001JD000779, 2002.

Dillon, M. B.: The chemical evolution of the Sacramento urban plume, Ph. D. thesis, 206 pp, University of California, Berkeley, 2002

Dillon, M. B., Lamanna, M. S., Schade, G. W., Goldstein, A. H., and Cohen, R. C.: Chemical evolution of the Sacramento urban plume: Transport and oxidation, J. Geophys. Res.-A., 107, 4045, doi:10.1029/2001JD000969, 2002.

Dreyfus, G. B., Schade, G. W., and Goldstein, A. H.: Observational constraints on the contribution of isoprene oxidation to ozone production on the western slope of the Sierra Nevada, CA, J. Geophys. Res.-A., 107, 4365, doi:10.1029/2001JD001490, 2002.

Farmer, D. K. and Cohen, R. C.: Observations of HNO_3, ΣAN an ΣPN and NO_2 fluxes: Evidence for rapid HO_x chemistry within a pine forest canopy, Atmos. Chem. Phys. Discuss., 7, 7087–7136, 2007, http://www.atmos-chem-phys-discuss.net/7/7087/2007/.

Fischer, M. L. and Littlejohn, D.: Ammonia at Blodgett Forest, Sierra Nevada, USA, Atmos. Chem. Phys. Discuss., 7, 14 139–14169, 2007.

Fountoukis, C., Sullivan, A., Weber, R., Vanreken, T., Fischer, M., Matias, E., Moya, M., Farmer, D. K., and Cohen, R. C.: Thermodynamic characterization of Mexico City aerosol during MILAGRO 2006, Atmos. Chem. Phys. Discuss., 7, 9203–9233, 2007, http://www.atmos-chem-phys-discuss.net/7/9203/2007/.

Gaffney, J. S. and Marley, N. A.: Measurements of peroxyacetyl nitrate at a remote site in the Southwestern United States: Tropopheric implications, Environ. Sci. Technol., 27, 1905–1910, 1993.

Goldstein, A. H., Hultman, N. E., Fracheboud, J. M., Bauer, M. R., Panek, J. A., Xu, M., Qi, Y., Guenther, A. B., and Baugh, W.: Effects of climate variability on the carbon dioxide, water, and sensible heat fluxes above a ponderosa pine plantation in the Sierra Nevada (CA), Agricultural and Forest Meteorology, 101, 113–129, 2000.

Hasson, A. S., Tyndall, G. S., and Orlando, J. J.: A product yield study of the reaction of HO_2 radicals with ethyl peroxy ($C_2H_5O_2$), acetyl peroxy ($CH_3C(O)O_2$), and acetonyl peroxy ($CH_3C(O)CH_2O_2$) radicals, J. Phys. Chem. A., 108, 5979–5989, 2004.

Herman, D. J., Halverson, L. J., and Firestone, M. K.: Nitrogen dynamics in an annual grassland: oak canopy, climate, and microbial population effects, Ecological Applications, 13, 593–604, 2003.

Hogrefe, C., Biswas, J., Lynn, B., Civerolo, K., Ku, J. Y., Rosenthal, J., Rosenzweig, C., Goldberg, R., and Kinney, P. L.: Simulating regional-scale ozone climatology over the eastern United States: model evaluation results, Atmos. Environ., 38, 2627–2638, 2004

Horowitz, L. W., Fiore, A. M., Milly, G. P., Cohen, R. C., Perring, A., Wooldridge, P. J., Hess, P. G., Emmons, L. K., and Lamarque, J.-F.: Observational constraints on the chemistry of isoprene over the Eastern U.S., J. Geophys. Res.-A., 112, D12S08, doi:10.1029/2006JD007747, 2007.

Kleinman, L., Lee, Y. N., Springston, S. R., Nunnermacker, L., Zhou, X. L., Brown, R., Hallock, K., Klotz, P., Leahy, D., Lee, J. H., and Newman, L.: Ozone formation at a rural site in the Southeastern United States, J. Geophys. Res.-A., 99, 3469–3482, 1994.

Kuhn, U., Andreae, M. O., Ammann, C., Araújo, A. C., Brancaleoni, E., Ciccioli, P., Dindorf, T., Frattoni, M., Gatti, L. V., Ganzeveld, L., Kruijt, B., Lelieveld, J., Lloyd, J., Meixner, F. X., Nobre, A. D., Pöschl, U., Spirig, C., Stefani, P., Thielmann, A., Valentini, R., and Kesselmeier, J.: Isoprene and monoterpene fluxes from Central Amazonian rainforest inferred from tower-based and airborne measurements, and implications on the atmospheric chemistry and the local carbon budget, Atmos. Chem. Phys., 7, 2855–2879, 2007, http://www.atmos-chem-phys.net/7/2855/2007/.

Kurpius, M. R., McKay, M., and Goldstein, A. H.: Annual ozone deposition to a Sierra Nevada ponderosa pine plantation, Atmos. Environ., 36, 4503–4515, 2002

Lamb, B., Guenther, A., Gay, D., and Westberg, H.: A national inventory of biogenic hydrocarbon emissions, Atmos. Environ., 21, 1695–1705, 1987.

Lefer, B. L., Talbot, R. W., and Munger, J. W.: Nitric acid and ammonia at a rural northeastern U.S. site, J. Geophys. Res.-A., 104, 1645–61, 1999.

Leung, L. R. and Gustafson, W. I.: Potential regional climate change and implications to US air quality, Geophys. Res. Lett., 32, L16711, doi:10.1029/2005GL022911, 2005.

Lopez, A., Barthomeuf, M. O., and Huertas, M. L.: Simulation of chemical processes occurring in an atmopheric boundary layer. Influence of light and biogenic hydrocarbons on the formation of oxidants., Atmos. Environ., 23, 1465–1478, 1989.

Murazaki, K. and Hess, P.: How does climate change contribute to surface ozone change over the United States?, J. Geophys. Res.-A., 111, D05301, doi:10.1029/2005JD005873, 2006

Murphy, J. G., Day, A., Cleary, P. A., Wooldridge, P. J., and Cohen, R. C.: Observations of the diurnal and seasonal trends in nitrogen oxides in the western Sierra Nevada, Atmos Chem. Phys., 6, 5321–5338, 2006a.

Murphy, J. G., Day, D. A., Cleary, P. A., Wooldridge, P. J., Millet, D. B., Goldstein, A. H., and Cohen, R. C.: The weekend effect within and downwind of Sacramento: Part 1. Observations of ozone, nitrogen oxides, and VOC reactivity, Atmos. Chem. Phys. Discuss., 6, 11 427–11 464, 2006b.

Murphy, J. G., Day, D. A., Cleary, P. A., Wooldridge, P. J., Millet, D. B., Goldstein, A. H., and Cohen, R. C.: The weekend effect within and downwind of Sacramento: Part 2. Observational evidence for chemical and dynamical contributions, Atmos. Chem. Phys. Discuss., 6, 11971-12019, 2006c, http://www.atmos-chem-phys-discuss.net/6/11971/2006/.

Olszyna, K. J., Bailey, E. M., Simonaitis, R., and Meagher, J. F.: O_3 and NO_y relationships at a rural site, Geophys. Res. Lett., 99, 14 557–14 563, 1994.

Olszyna, K. J., Luria, M., and Meagher, J. F.: The correlation of temperature and rural ozone levels in southeastern USA, Atmos. Environ., 31, 3011–3022, 1997.

Parrish, D. D., Norton, R. B., Bollinger, M. J., Liu, S. C., Murphy, P. C., Albritoon, D. L., Fehsenfeld, F. C., and Heubert, B. J.: Measurements of HNO_3 and NO_3 particulates at a rural site in the Colorado mountains, J. Geophys. Res.-A., 91, 5379–5393, 1986.

Ren, X., Olson, J. R., Crawford, J. H., Brune, W. H., Mao, J., Long, R. B., Chen, G., Avery, M. A., Sachse, G. W., Barrick, J. D., Diskin, G., Huey, L. G., Fried, A., Cohen, R. C., Heikes, B., Wennberg, P. O., Singh, H. B., Blake, D. R., and Shetter, R. E.: HOx chemistry during INTEX-A 2004: Observation, model calculation, and comparison with previous studies., J. Geophys. Res.-A., 113, D05310, doi:10.1029/2007JD009166, 2008.

Rosen, R. S., Wood, E., Wooldridge, P. J., Thornton, J. A., Kuster, B., Williams, E. J., Jobson, B. T., and Cohen, R. C.: Observations of total alkyl nitrates during Texas Air Quality Study 2000: Implications for O_3 and alkyl nitrate photochemistry., J. Geophys. Res.-A., 107, D07303, doi:10.1029/2003JD004227, 2004.

Rubin, J. I., Kean, A. J., Harley, R. A., Millet, D. B., and Goldstein, A. H.: Temperature dependence of volatile organic compound evaporative emissions from motor vehicles, J. Geophys. Res.-A., 111, D03305, doi:10.1029/2005JD006458, 2006.

Sander, S. P.: Chemical kinetics and photochemical data for use in atmospheric studies, Evaluation number 15; NASA Panel for Data Evaluation, edited, National Aeronautics and Space Administration; Jet Propulsion Laboratory California Institute of Technology, Pasadena, California, 2006.

Schade, G. W. and Goldstein, A. H.: Fluxes of oxygenated volatile organic compounds from a ponderosa pine plantation, J. Geophys. Res.-A., 106, 3111–3123, 2001.

Schrimpf, W., Linaerts, K., Muller, K. P., Koppmann, R., and Rudolph, J.: Peroxyacetyl nitrate (PAN) measurements during the POPCORN campaign, J. Atmos. Chem., 31, 139–159, 1998.

Seaman, N. L., Stauffer, D. R., and Lariogibbs, A. M.: A multiscale 4-dimensional data assimilation system applied in the San-Joaquin Valley during Sarmap .1. Modeling design and basic

performance-characteristics, J. Appl. Meteorol., 34, 1739–1761, 1995.

Sillman, S. and Samson, P. J.: Impact of temperature on oxidant photochemistry in urban, polluted rural and remote environments, J. Geophys. Res.-A., 100, 11 497–11 508, 1995.

Steiner, A. L., Tonse, S., Cohen, R. C., Goldstein, A. H., and Harley, R. A.: Influence of future climate and emissions on regional air quality in California, J. Geophys. Res.-A., 111, D18303, doi:10.1029/2005JD006935, 2006.

Stevenson, D., Doherty, R., Sanderson, M., Johnson, C., Collins, B., and Derwent, D.: Impacts of climate change and variability on tropospheric ozone and its precursors, Faraday Discussions, 130, 41–57, 2005.

Stickler, A., Fischer, H., Bozem, H., Gurk, C., Schiller, C., Martinez-Harder, M., Kubistin, D., Harder, H., Williams, J., Eerdekens, G., Yassaa, N., Ganzeveld, L., Sander, R., and Lelieveld, J.: Chemistry, transport and dry deposition of trace gases in the boundary layer over the tropical Atlantic Ocean and the Guyanas during the GABRIEL field campaign, Atmos. Chem. Phys. Discuss., 7, 4781–4855, 2007, http://www.atmos-chem-phys-discuss.net/7/4781/2007/.

Stump, F. D., Knapp, K. T., Ray, W. D., Snow, R., and Burton, C.: The composition of motor-vehicle organic emissions under elevated-temperature summer driving conditions (75-degrees-F to 105-degrees-F), Journal of the Air and Waste Management Association, 42, 152–158, 1992.

Tan, D., Faloona, I., Simpas, J. B., Brune, W., Shepson, P. B., Couch, T. L., Sumner, A. L., Carroll, M. A., Thornberry, T., Apel, E., Riemer, D., and Stockwell, W.: HO_x budgets in a deciduous forest: Results from the PROPHET summer 1998 campaign, J. Geophys. Res.-A., 106, 24407–24427, 2001.

Thornton, J. A., Wooldridge, P. J., and Cohen, R. C.: Atmospheric NO_2: In situ laser-induced fluorescence detection at parts per trillion mixing ratios, Anal. Chem., 72, 528–539, 2000.

Thornton, J. A., Wooldridge, P. J., Cohen, R. C., Martinez, M., Harder, H., Brune, W. H., Williams, E. J., Fehsenfeld, F. C., Hall, S. R., Shetter, R. E., Wert, B. P., and Fried, A.: Observations of ozone production rates as a function of NO_2 abundances and HO_x production rates in the Nashville urban plume, J. Geophys. Res.-A., 107, 4146, doi:10.1029/2001JD000932, 2002.

Trainer, M., Buhr, M. P., Curran, C. M., Fehsenfeld, F. C., Hsie, E. Y., Liu, S. C., Norton, R. B., Parrish, D. D., Williams, E. J., Gandrud, B. W., Ridley, B. A., Shetter, J. D., Allwine, E. J., and Westberg, H. H.: Observations and modeling of the reactive nitrogen photochemistry at a rural site, J. Geophys. Res.-A., 96, 3045–3063, 1991.

UCAR/NCAR/ACD: Tropospheric Ultraviolet and Visible (TUV) Radiation Model, http://cprm.acd.ucar.edu/Models/TUV/, 2006.

van Dijk, S. M., Gut, A., Kirkman, G. A., Meixner, F. X., Andreae, M. O., and Gomes, B. M.: Biogenic NO emissions from forest and pasture soils: Relating laboratory studies to field measurements, J. Geophys. Res.-A., 107, 8058, doi:10.1029/2001JD000358, 2002.

Welstand, J. S., Haskew, H. H., Gunst, R. F., and Bevilacqua, O. M.: Evaluation of the effects of air conditioning operation and associated environmental conditions on vehicle emissions and fuel economy, Tech. Pap. Ser., 2003-01-2247, 2003.

Wiedinmyer, C., Greenberg, J., Guenther, A., Hopkins, B., Baker, K., Geron, C., Palmer, P. I., Long, B. P., Turner, J. R., Petron, G., Harley, P., Pierce, T. E., Lamb, B., Westberg, H., Baugh, W., Koerber, M., and Janssen, M.: Ozarks Isoprene Experiment (OZIE): Measurements and modeling of the "isoprene volcano", J. Geophys. Res.-A., 110, D18307, doi:10.1029/2005JD005800, 2005.

Williams, E. J., Guenther, A., and Fehsenfeld, F. C.: An inventory of nitric-oxide emissions from soils in the United-States, J. Geophys. Res.-A., 97, 7511–7519, 1992.

Williams, E. J., Roberts, J. M., Baumann, K., Bertman, S. B., Buhr, S., Norton, R. B., and Fehsenfeld, F. C.: Variations in NO_y composition at Idaho Hill, Colorado, J. Geophys. Res.-A., 102, 6297–6314, 1997

Zhang, Q., Carroll, J. J., Dixon, A. J., and Anastasio, C.: Aircraft measurements of nitrogen and phosphorus in and around the Lake Tahoe Basin: Implications for possible sources of atmospheric pollutants to Lake Tahoe, Environ. Sci. Technol., 36, 4981–4989, 2002.